Project no. TREN/07/FP6AE/S07.71574/037180 iFly

iFly

Safety, Complexity and Responsibility based design and validation of highly automated Air Traffic Management

Specific Targeted Research Projects (STREP)

Thematic Priority 1.3.1.4.g Aeronautics and Space

iFly Deliverable D7.2d

Periodic Boundary Condition in Simulating Large Scale Airborne Self Separation Airspace

Version: 1.0

by A. Goswami (TWEN), G.J. Bakker & H.A.P. Blom (NLR)

Due date of deliverable: 22 January 2009
Actual submission date: 5 March 2010

Start date of project: 22 May 2007 Duration: 51 months

Project co-funded by the European Commission within the Sixth Framework Programme (2002-2006)		
Dissemination Level		
PU	Public	X
PP	Restricted to other programme participants (including the Commission Services)	
RE	Restricted to a group specified by the consortium (including the Commission Services)	
CO	Confidential, only for members of the consortium (including the Commission Services)	

DOCUMENT CONTROL SHEET

Title of document:	Periodic Boundary Condition in Large Scale Airborne Self Separation Airspace
Authors of document:	Anindya Goswami, G.J. (Bert) Bakker and Henk A.P. Blom
Deliverable number:	D7.2d
Project acronym:	iFly
Project title:	Safety, Complexity and Responsibility based design and validation of highly automated Air Traffic Management
Project no.:	TREN/07/FP6AE/S07.71574/037180 iFly
Instrument:	Specific Targeted Research Projects (STREP)
Thematic Priority:	1.3.1.4.g Aeronautics and Space

DOCUMENT CHANGE LOG

Version#	Issue Date	Sections affected	Relevant information
0.0	30-04-2008	All	A draft by Jaroslav Krystul
0.1	09-03-2009	All	A draft by Anindya Goswami
0.2	21-03-2009	All	A draft by Bert Bakker
0.3	29-04-2009	All	NNE criteria is introduced
0.4	09-06-2009	All	Revised thoroughly with new scenarios and a section of numerical evaluation
0.5	18-08-2009	All	An appendix is included
0.6	13-11-2009	All	A new section on width of PBC cell is added
0.7	22-12-2009	4, 5	Sharper sufficient condition is suggested
0.8	15-01-2010	1,4,5	The draft is revised
1.0	11-04-2010	All	EC review comment incorporated

Version 0.7		Organisation	Signature/Date
Authors	Anindya Goswami	TWEN	
	Bert Bakker	NLR	
	Henk Blom	NLR	
Internal reviewers	Arun Bagchi	TWEN	
	Jaroslav Krystul	TWEN	
External reviewers	Uwe Voelckers	Independent	

Periodic Boundary Condition Based Simulation of Large Scale Airborne Self Separation Airspace

Abstract

In order to simulate a large 3D airspace with a very large number of airborne self separating aircraft we make use of a Periodic Boundary Condition (PBC) consisting of a rectangular 3D box. Infinitely many of these boxes are packing the 3D airspace, and in each 3D box a fixed number N of aircraft is flying. Then only N aircraft have to be simulated in order to get hold on the collision risk in a homogeneously dense 3D airspace. Although PBC is a common approach in molecular dynamics simulation, little is known about choosing a sufficiently large PBC. In this report we develop some requirements on the minimal size of the 3D box.

1 Introduction

In [1], a large 3D airspace with a very large number of airborne self separating aircraft have been simulated by making use of a Periodic Boundary Condition (PBC) [4]. Imposing a proper PBC on the 3D airspace eases the matter in the following way:

- Implicitly, it assumes that the aircraft in a 3D airspace are flying in a particular pattern such that the 3D airspace can be partitioned into identically cells, and with identical aircraft-trajectories evolving in each of these cells.
- Under this implicit assumption, it is sufficient to simulate the trajectories in only one cell, and each time that one of the aircraft trajectories leaves this cell, it enters the same cell at the opposite side of the cell.

The specific PBC cell used in [1] is a rectangular 3D box, infinitely many of them which are packing a virtually infinite 3D airspace. In each 3D box, N airborne self separating aircraft are flying. This way, one only needs to simulate N aircraft in one box, in order to mimic a simulation of infinitely many aircraft in an infinite 3D airspace. In [1] the maximum number of aircraft that have been simulated without running into computer memory problems was eight; hence in [1] N=8. Subsequently, in [1] the size of the 3D box has been varied in order to vary the aircraft density in the 3D airspace.

It is important to note that the collision probability of an aircraft in random traffic with PBC may differ from that in random traffic without PBC. Fortunately this error can be made arbitrarily small by making the sizes of the boxes sufficiently large.

Although the use of PBC is a well known approach in molecular dynamics simulation [4], little is known about choosing a sufficiently large PBC cell. Therefore in [1] the size of the 3D box has been chosen rather arbitrarily. In [1] it has been observed that sometimes a rare event happened in the simulation which was due to the limited height of the 3D box. None of such events have been observed that were caused by the limited width of the 3D box. Because events caused by the limited size of the 3D box can properly be identified, the potential errors caused by a too small sized 3D box can be kept under control [1]. Nevertheless we also want to develop proper theory in order to better understand under which conditions the size of the 3D box is large enough. The

objective of this report is to derive bounds on the size of the 3D boxes under the airborne self separation concept considered in [1].

This report is arranged as follows. In Section 2 the use of *PBC* in dense random traffic airspace is revisited with mathematical description. The notion of sufficiently large *PBC* cell is also introduced in a very general set-up. In Section 3 and 4 a sufficiently large rectangular box is studied. For some specific scenarios the minimum height of this rectangular box is derived in Section 3. And the minimum width of this rectangular box is derived in Section 4. In Section 5 we illustrate the results by some numerical evaluations. Section 6 contains some concluding remarks. BADA performance data of several aircraft types has been used [5], details of which are given in Appendix A.

2 Periodic Boundary Condition in Random Traffic Airspace

The concept of primitive cell of a lattice plays a key role in the construction of periodic boundary. We recall the definition below.

Definition 2.1 *Let $\mathcal{L}$ be a lattice in $\mathbb{R}^3$ with translational symmetries. Let $\{\vec{a_1}, \vec{a_2}, \vec{a_3}\}$ be a set of independent lattice vectors of smallest magnitude. A primitive cell $C \subset \mathbb{R}^3$ is given by*

$$C = \{\vec{x} = \alpha_1\vec{a_1} + \alpha_2\vec{a_2} + \alpha_3\vec{a_3} \mid \alpha_i \in [0, 1), i = 1, 2, 3\}.$$

From the definition of primitive cell the following result follows.

Theorem 2.2 *For $x \in \mathbb{R}^3$, there exists a unique set of integers $\{k_1, k_2, k_3\}$ such that $x \in C + k_1\vec{a_1} + k_2\vec{a_2} + k_3\vec{a_3}$. In other words, the whole space can be covered by disjoint translated copies of the primitive cell.*

The method of periodic boundary condition is common in molecular dynamics. The following subsection explains how the *PBC* arises in airborne self separation traffic simulation modelling.

2.1 Construction of Periodicity

Fix one three dimensional lattice in the airspace. Make N number of copies of that lattice. Assume each node of each lattice as an aircraft. Also assume that each of the N lattices are following random translational trajectories independent to each other, keeping relative position of all nodes unaltered in a single lattice. Now consider a cell or container in the airspace having same shape, size and orientation of those of the *primitive cell* (see Definition 2.1) of the lattice. Fill the airspace with the translated copies of this cell as in Theorem 2.2. It follows that the following consequences take place.

- Always there are exactly N aircraft (or nodes of lattices) in each cell at a time.
- The relative positions and trajectories of aircraft in one cell is identically same to those in other cells.
- Each of the N number of aircraft in a single lattice are driven by independent noises.
- If an aircraft leaves the cell through a particular bounding face immediately another enters the cell through the opposite face (see Figure 1).

- Aircraft flying within some distance d_c of a boundary interact with aircraft in an adjacent copy of the cell, or, equivalently, with aircraft near the opposite boundary - a wraparound effect

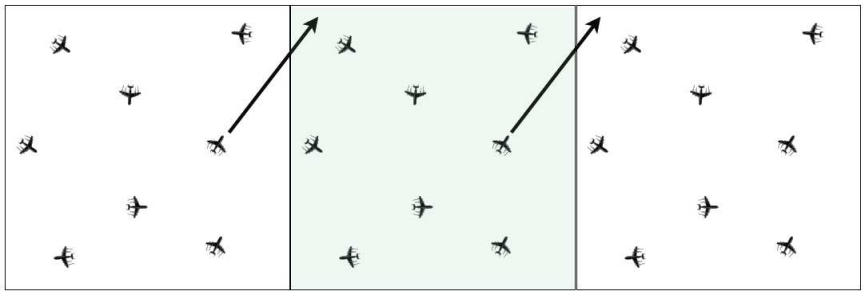

Figure 1: *PBC* in random air traffic modeling applied on rectangular 2D-cell

Hence to take account of the full airspace it is sufficient to model only one cell containing N aircraft having trajectories with independent noises and satisfy appropriate boundary conditions.

2.2 Formulation of Periodic Boundary Condition

In the sequel of this report we consider a particular type of *PBC* where the cells are rectangular in 3-dimensions as in [1]. To this end the generating set $\{\vec{a}_1, \vec{a}_2, \vec{a}_3\}$ of the lattice is a set of orthogonal vectors with $\vec{a}_3$ vertical to the Earth surface. After fixing an appropriate reference frame, the vectors can be chosen as $\vec{a}_1 = [d, 0, 0], \vec{a}_2 = [0, d, 0]$ and $\vec{a}_3 = [0, 0, h]$. Therefore the horizontal position of an aircraft copy in the neighboring upper or lower cell is the same as original (i.e. no horizontal shift for copies) and the speeds are the same as original, only height is shifted.

The wrap around effect of the periodic boundaries must be taken into account in both the integration of the equations of the motion and the interaction computations. After each integration step the coordinates must be examined, and if an aircraft is found to have flown outside the cell its coordinates must be adjusted to bring it back inside. Therefore, once the size and the shape of the cell is suitably chosen, the corresponding *PBC* needs to be formulated appropriately. In this report we consider rectangular shapes of PBC only in 2 or 3 dimensions. Here is an example of boundary condition corresponding to a rectangular box cell having horizontal side lengths d and vertical height h.

Let (x, y, z) be the coordinate of an aircraft in a rectangular box cell. The boundary condition for this aircraft can be written as follows

$$
\begin{aligned}
z &\leftarrow \begin{cases} z-h & \text{if} \quad z \geq h \\ z+h & \text{if} \quad z < 0 \end{cases} \\
y &\leftarrow \begin{cases} y-d & \text{if} \quad y \geq d \\ y+d & \text{if} \quad y < 0 \end{cases} \\
x &\leftarrow \begin{cases} x-d & \text{if} \quad x \geq d \\ x+d & \text{if} \quad x < 0. \end{cases}
\end{aligned}
$$

Remark 2.3 *In the above discussion it becomes clear that the choice of size and orientation of a rectangular box cell depends on the lattice structure or periodicity of the air traffic model under* PBC *and vise versa. Therefore a particular geometry of cell corresponds to a particular* PBC.

Thus, in order to specify a particular PBC *we would specify the corresponding primitive cell now onward.*

In order to investigate the events such as collision, the choice of orientation of a rectangular cell is immaterial. Therefore, the cell can be chosen with one face horizontal without the loss of generality. But the size of the cell has a direct relation to the relative positions of the aircraft, which has a significant impact on the occurrence of an event like a Mid Air Collision (MAC). In the next subsection we address few important consequences of periodic structure / cell size parameters.

2.3 Consequences of PBC in [1]

In this section we explain some consequences of applying PBC in [1]. The following notations are important in the subsequent discussions.

Notation 2.4 *Let N be the number of aircraft in each cell and V the size of the cell. Then $\rho := \frac{N}{V}$ is the traffic density.*

From the definition of ρ it is evident that a fixed value of ρ can be maintained with fewer number of aircraft N by simply decreasing the size V of the cell. And thus the computation can be faster. But the value of N cannot be too small as well. Because, for a given fixed ρ, V is minimum for $N = 1$. In this extreme case the relative position of all the aircraft in the whole air traffic model are fixed, hence a MAC does not happen. For $N = 2$, only collisions between two aircraft are considered. In order to simulate chain reactions we need $N >> 1$.

Example 2.5 *In [1] $N = 8$ has been chosen to include the possibility of chain reactions in air traffic. Subsequently the baseline traffic density value is set to be* 0.008 *aircraft per Nm^3 which is* 2.5 *times the level of one of the busiest en-route sectors in Europe in 1999. To mimic this density, rectangular box PBC of* $40Nm \times 40$ *Nm and* $4000ft$ *height.*

In [1] there have been a few encounters observed where a feasible resolution by ASAS maneuver caused a new encounter between one and a copy of the other aircraft. This typically is an event due to a too small PBC cell size. An example from [1] of this type of undesired event is the following.

Example 2.6 *(example identified during MC simulations in [1]). The cell specifications are given in Example 2.5. In [1] for this example a sequential MC simulation is performed with* $10,000$ *particles and five different MAC are observed. Among these five MAC one is of the following type: at quite a late moment a conflict of aircraft #1 with aircraft #2 is solved through a fast climb by aircraft #1 and this created a MAC with a copy of #2 in a neighboring upper cell.*

In order to get grip on these undesired conflicts using PBC, we define the following criterion on *PBC*.

Definition 2.7 *Let C be the cell corresponding to a given* PBC*. Let τ be a stopping time w.r.t the prediction model of the aircraft trajectory under the given* PBC*, based on the information at $t = 0$. We assume that under this* PBC *there is a class $\mathcal{E}$ of encounters (detected at time $t = 0$) that has a predicted resolution by a set of maneuver with constraint set $\mathcal{M}$ without creating a new encounter between one and a copy of the other aircraft during $[0, \tau]$. Then we call the class $\mathcal{E}$ to satisfy* No New Encounter *criteria with respect to $(C, \mathcal{M}, \tau)$. In short, we say $\mathcal{E}$ satisfies* NNE *w.r.t $(C, \mathcal{M}, \tau)$. Equivalently we also say that the* PBC *cell C is sufficiently large w.r.t $(\mathcal{E}, \mathcal{M}, \tau)$.*

In the next section we deal with some examples where we show the existence of a nonempty $\mathcal{E}$ satisfying *NNE* w.r.t a particular choice of $(C, \mathcal{M}, \tau)$. From the definition it is clear that a *PBC* cell C being sufficiently large for a particular $(\mathcal{E}, \mathcal{M}, \tau)$ is not ensured to be sufficiently large for $(\mathcal{E}', \mathcal{M}, \tau)$ where $\mathcal{E}'$ is a class of encounters larger than $\mathcal{E}$. Therefore, while trading off as in Example 2.5 we also search for a *PBC* which allows a reasonably large class of encounters to satisfy the *NNE* criteria.

2.4 Gradation of *PBC* by ASAS Conflict Detection and Resolution

In order to predict the trajectory we assume a linear trajectory prediction. Based on predicted relative positions the ASAS conflicts are detected. Let the linear prediction be done at $t = 0$ and let $\tilde{s}_t^{ij}$ represent the predicted 2D horizontal position of aircraft i relative to aircraft j. Let R and H_{sep} be the horizontal and vertical separation minima respectively.

Three horizontal stopping times are relevant for conflict detection (and are also used for resolution):

- the first time for which there is a horizontal predicted conflict (conflict in):
  $\tau_{in}^{ij} = \inf\{t; \|\tilde{s}_t^{ij}\| \leq R\}$
- the time of horizontal predicted miss distance :
  $\tau_{min}^{ij} = \inf\{t_0 : t_0 \text{ is a local minima of the predicted map } t \mapsto \|\tilde{s}_t^{ij}\|\}$
- the first time for which horizontal predicted conflict is ended (conflict out):
  $\tau_{out}^{ij} = \inf\{t > \tau_{min}^{ij}; \|\tilde{s}_t^{ij}\| > R\}$.

Based on these stopping times we may define three different categories of *PBC* related to the sufficiency of its size w.r.t a given $\mathcal{E}$ and $\mathcal{M}$. The gradations are as follows.

Grade 1 *PBC* : If a given *PBC* cell C is sufficiently large w.r.t $(\mathcal{E}, \mathcal{M}, \tau_{in}^{ij})$ for any pair of aircraft i and j having an initial encounter in the class $\mathcal{E}$ then we say that C corresponds to a *grade 1 PBC* w.r.t $(\mathcal{E}, \mathcal{M})$.

Grade 2 *PBC* : If a given *PBC* cell C is sufficiently large w.r.t $(\mathcal{E}, \mathcal{M}, \tau_{min}^{ij})$ for any pair of aircraft i and j having an initial encounter in the class $\mathcal{E}$ then we say that C corresponds to a *grade 2 PBC* w.r.t $(\mathcal{E}, \mathcal{M})$.

Grade 3 *PBC* : If a given *PBC* cell C is sufficiently large w.r.t $(\mathcal{E}, \mathcal{M}, \tau_{out}^{ij})$ for any pair of aircraft i and j having an initial encounter in the class $\mathcal{E}$ then we say that C corresponds to a *grade 3 PBC* w.r.t $(\mathcal{E}, \mathcal{M})$.

3 Issues Related to the Height of the Rectangular Box

In the previous sections we have introduced the notion of sufficiently large *PBC* and we also obtain a gradation of *PBC* corresponding to its level of sufficiency. These gradations are defined for any arbitrary scenario. But the definitions do not suggest a particular methodology for grading a *PBC* on considering a particular scenario. We address this problem in this section, and we derive criteria regarding the height of the rectangular box in order to obtain a sufficiently large *PBC* cell. We derive sufficient vertical heights of the rectangular box for two vertical resolution scenarios. The first scenario assumes two aircraft to change height whereas the second scenario assumes only one of the aircraft to change height.

3.1 Assumptions of Scenario 1

We consider encounters between a pair of aircraft at the same flight level where both aircraft change heights. Here we state the assumptions.

Assumption on initial state

A.0 Let two aircraft, #1 and #2 fly at the same flight level and on a head-on course with equal speeds in opposite directions.

Let L be the distance between them at time $t = 0$ when ASAS maneuver is started. i.e., $\|\tilde{s}_0^{12}\| = L$. Let $V_\parallel$ be the absolute value of their horizontal velocities.

Assumptions on maneuver

A.1 #1 and #2 start vertical resolution simultaneously at $t = 0$.

A.2 #1 climbs with constant vertical speed $V_\perp$ and #2 descends with constant vertical speed $-V_\perp$.

A.3 No level off, i.e aircraft keep climbing/descending.

A.4 Upper bound on $V_\perp$ i.e., $V_\perp \leq V_\perp^{max}$ with $V_\perp^{max} > 0$.

Additional assumptions on initial state

A.5 Upper and lower bounds on horizontal speed, i.e., $V_\parallel^{min} \leq V_\parallel \leq V_\parallel^{max}$, with $V_\parallel^{max} \geq V_\parallel^{min} > 0$.

A.6 $L - \frac{2H_{sep}}{V_\perp^{max}} V_\parallel \geq R$.

Let $\mathcal{E}_1$ denotes the class of all encounters in which the initial state (relative positions and velocities when the conflict resolution maneuver is taken) satisfies A0, A.5 and A.6. Or in other words

$\mathcal{E}_1 = \{(\tilde{s}_0^{12}, \tilde{v}_0^1, \tilde{v}_0^2) \in \mathbb{R}^3 \times \mathbb{R}^3 \times \mathbb{R}^3 \mid \tilde{s}_0^{12} = L\vec{e}, \tilde{v}_0^1 = -\tilde{v}_0^2 = V_\parallel \vec{e}, \vec{e} \perp \vec{a}_3, \|\vec{e}\| = 1, V_\parallel^{min} \leq V_\parallel \leq V_\parallel^{max}$ and $L - \frac{2H_{sep}}{V_\perp^{max}} V_\parallel \geq R\}$ where $\tilde{v}_t^i$ denotes the predicted velocity of ith aircraft at instant t.

Lemma 3.1 *If maneuver A.1-A.4 is taken, we have*

$$\min_{\mathcal{E}_1}(L - R) = \frac{2H_{sep}}{V_\perp^{max}} V_\parallel^{min}.$$

Proof : Since A.5 and A.6 are satisfied under $\mathcal{E}_1$, we have

$$L - R \geq \frac{2H_{sep}}{V_\perp^{max}} V_\parallel \geq \frac{2H_{sep}}{V_\perp^{max}} V_\parallel^{min}.$$

Again the triplet $((R + \frac{2H_{sep}}{V_\perp^{max}} V_\parallel^{min})\vec{e}, V_\parallel^{min}\vec{e}, -V_\parallel^{min}\vec{e})$ is in $\mathcal{E}_1$. Hence the result follows. ∎

In the subsequent discussion, the class $\mathcal{E}_1$ is termed as the class of usual encounters.

3.2 Predicted ASAS Vertical Instantaneous Resolution under scenario 1

Under the assumptions A.1, A.2 and A.3 on manoeuver constraint both aircraft #1 and #2, having an usual encounter, are doing resolution at the same time t=0, and keep climbing/descending. For scenario 1 and ASAS application considered, the constant vertical speed $V_\perp$ should be such that the vertical separation at $\tau_{in}^{1,2}$ is a prescribed value H_{sep} in case the other aircraft is not doing a resolution.
This suggests $V_\perp$ to be equal to $H_{sep}/\tau_{in}^{1,2}$. But the maneuver constraint A.4 puts an upper bound of $V_\perp$. Thus we get

$$V_\perp = \min\left\{V_\perp^{max}, \frac{2H_{sep}}{L-R}V_\parallel\right\}$$

since, $\tau_{in}^{1,2} = \frac{L-R}{2V_\parallel}$. Again since we consider the encounters with initial condition A.6, we finally obtain

$$V_\perp = \frac{2H_{sep}}{L-R}V_\parallel.$$

Since the predicted accelerations are assumed to be zero during the resolution, we obtain linear predicted trajectories of the aircraft. Thus we can draw a figure with rectilinear predicted paths. The Figure 2 demonstrates the predicted resolution. From the Figure 2 it follows that

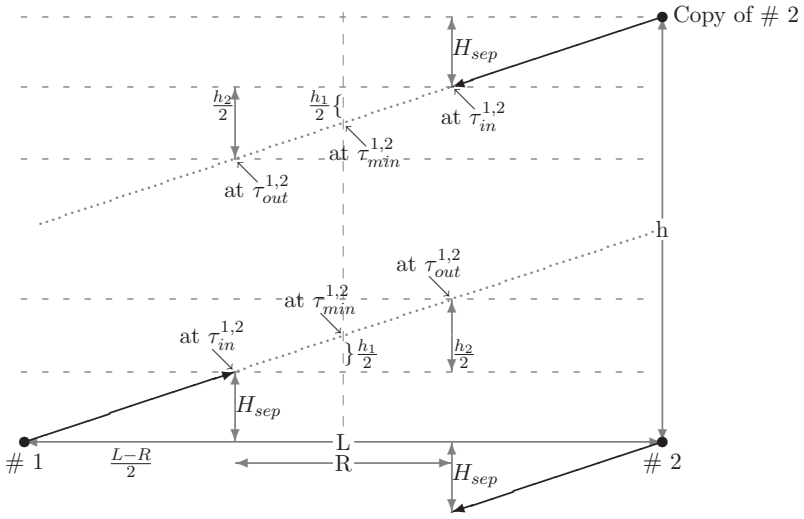

Figure 2: Side view of ASAS vertical resolution (predictions)

$$\frac{h_1}{2} \div \frac{R}{2} = H_{sep} \div \frac{L-R}{2} \quad \Rightarrow \quad h_1 = \frac{2H_{sep}R}{L-R}$$

and

$$\frac{h_2}{2} \div R = H_{sep} \div \frac{L-R}{2} \quad \Rightarrow \quad h_2 = \frac{4H_{sep}R}{L-R}.$$

3.3 Evaluation of Minimal Box Height for Each Grade under scenario 1

Grade 1: Since the (predicted) horizontal positions and speeds are the same for the copies (see Figure 2), the horizontal stopping times for the copies are the same as for the original aircraft. Hence it suffices to consider the aircraft pair #1 and copy of #2 at time $t = \tau_{in}^{1,2}$ and we must have

(predicted) vertical separation at that time. This is a necessary and suficient condition for grade 1 *PBC*. From the Figure 2 we get

$$h - 2H_{sep} \geq H_{sep}.$$

Hence,

$$h \geq 3H_{sep}.$$

Grade 2: As earlier it suffices to consider the copy of #2 at time $t = \tau_{min}^{1,2}$ and we must have (predicted) vertical separation at that time for all usual encounters to obtain a grade 2 *PBC*, i.e.,

$$\min_{\mathcal{E}_1}(h - 2H_{sep} - 2\frac{h_1}{2}) \geq H_{sep}.$$

Therefore,

$$\begin{aligned} h &\geq 3H_{sep} + \max_{\mathcal{E}_1} \frac{2H_{sep}R}{L-R} \\ &= 3H_{sep} + \frac{2H_{sep}R}{\min_{\mathcal{E}_1}(L-R)} \\ &= 3H_{sep} + \frac{V_{\perp}^{max}}{V_{\parallel}^{min}}R. \quad [\text{ From Lemma 3.1}] \end{aligned}$$

Hence a necessary and sufficient high value of h to obtain a *PBC* of grade 2 must satisfy

$$h \geq 3H_{sep} + \frac{V_{\perp}^{max}}{V_{\parallel}^{min}}R.$$

Grade 3: As earlier we consider the pair #1 and the copy of #2 at time $t = \tau_{out}^{1,2}$. From the Figure 2 we get the following necessary and sufficient condition for grade 3 *PBC*

$$\min_{\mathcal{E}_1}(h - 2H_{sep} - 2\frac{h_2}{2}) \geq H_{sep}.$$

Hence,

$$\begin{aligned} h &\geq 3H_{sep} + \max_{\mathcal{E}_1} \frac{4H_{sep}R}{L-R} \\ &= 3H_{sep} + \frac{4H_{sep}R}{\min_{\mathcal{E}_1}(L-R)} \\ &= 3H_{sep} + \frac{V_{\perp}^{max}}{V_{\parallel}^{min}}2R. \quad [\text{ from Lemma 3.1}] \end{aligned} \tag{3.1}$$

Remark 3.2 *It is clear from the above discussion that the conditions on rectangular box height obtained for all three different grades are necessary as well as sufficient. In view of the tradeoffs discussed in Subsection 2.3, we are interested in the minimum height fulfilling the conditions for respective grades. We also note that:* minimum height for grade1 *PBC* $\leq$ minimum height for grade 2 *PBC* $\leq$ minimum height for grade 3 *PBC*. *Let the minimum height for grade 3* PBC *be denoted by* $h_{\min}$. *Thus if for a rectangular box the height* h *needs to be larger than* $h_{\min}$, *the corresponding* PBC *is sufficiently large under A.0-A.6 and for all three horizontal stopping times.*

3.4 Scenario 2 and Minimal Box Height

In this subsection we consider scenario 2 in which only one of the aircraft is assumed to change height, and we show how this influences the minimum box height characterization in subsection 3.1-3.3. This scenario 2 satisfies A.0 and A.3-A.6 but maneuver assumptions A.1 and A.2 are replaced by by the following assumptions:

A1′ #1 start vertical resolution at $t = 0$ but #2 does not take any resolution.

A2′ #1 climbs with constant vertical speed $V_\perp$ and #2 keeps flying horizontally with same horizontal speed.

Because we assume that scenario 2 obeys assumptions A.3-A.6, we have $V_\perp = \frac{2H_{sep}}{L-R}V_\parallel$ and obtain linear predicted trajectories of the aircraft as before. Figure 3 demonstrates the predicted resolution.

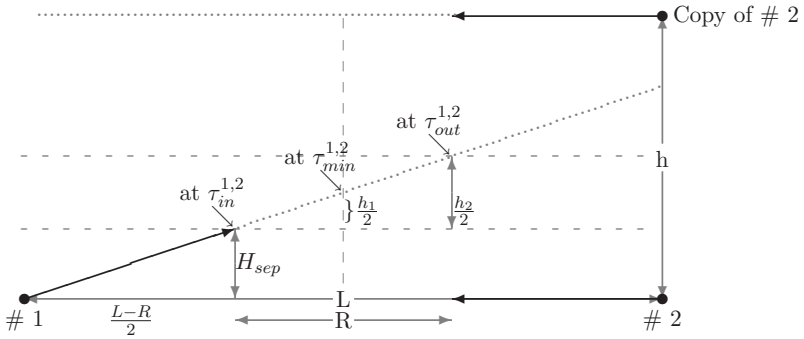

Figure 3: Side view of ASAS vertical resolution (predictions)

It is important to note that for this scenario the value of h_1 and h_2 are unchanged and the Lemma 3.1 still holds. The calculation of the box height for this scenario is given below.

Grade 1: As before we must have (predicted) vertical separation at $t = \tau_{in}^{1,2}$ between the aircraft pair #1 and copy of #2. From the Figure 3 we get

$$h - H_{sep} \geq H_{sep}.$$

Hence the necessary and sufficient height for grade 1 *PBC* is

$$h \geq 2H_{sep}.$$

Grade 2: As earlier it suffices to consider the copy of #2 at time $t = \tau_{min}^{1,2}$ and we must have (predicted) vertical separation at that time for all usual encounters, i.e.,

$$\begin{aligned}
\min_{\mathcal{E}_1}(h - H_{sep} - \frac{h_1}{2}) &\geq H_{sep} \\
h &\geq 2H_{sep} + \max_{\mathcal{E}_1} \frac{H_{sep}R}{L-R} \\
&= 2H_{sep} + \frac{H_{sep}R}{\min_{\mathcal{E}_1}(L-R)} \\
&= 2H_{sep} + \frac{V_\perp^{max}}{2V_\parallel^{min}}R. \quad [\text{ from Lemma 3.1}]
\end{aligned}$$

Hence a necessary and sufficient high value of h to obtain a *PBC* of grade 2 satisfies

$$h \geq 2H_{sep} + \frac{V_{\perp}^{max}}{2V_{\parallel}^{min}} R.$$

Grade 3: As earlier we consider the pair #1 and the copy of #2 at time $t = \tau_{out}^{1,2}$. From the Figure 2 we get

$$\min_{\mathcal{E}_1}(h - H_{sep} - \frac{h_2}{2}) \geq H_{sep}.$$

Hence a *PBC* of grade 3 is achieved if and only if

$$\begin{aligned} h &\geq 2H_{sep} + \max_{\mathcal{E}_1} \frac{2H_{sep}R}{L-R} \\ &= 2H_{sep} + \frac{2H_{sep}R}{\min_{\mathcal{E}_1}(L-R)} \\ &= 2H_{sep} + \frac{V_{\perp}^{max}}{V_{\parallel}^{min}} R. \quad [\text{ from Lemma 3.1}] \end{aligned} \tag{3.2}$$

3.5 Scenarios 1 and 2 with Heterogeneous Aircraft

The bounds on vertical and horizontal velocities (defined in A.4 and A.5) appear in the expression of minimum necessary rectangular box height derived in earlier subsections. Clearly, these parameters not only depend on the air traffic model under consideration but on the individual aircraft types as well. In particular the value of $\frac{V_{\perp}^{max}}{V_{\parallel}^{min}}$ ranges roughly from 0.05 to 0.08 depending on the aircraft type (see Appendix A). While specifying the *usual encounters* in subsection 3.1, so far we have ignored the heterogeneity of the aircraft and have assumed all the aircraft are of same type.

If we allow the encountering aircraft to be of heterogeneous type we should replace A.4, A.5 and A.6 by the following set of assumptions:

A.4′ Aircraft of ith type has an upper bound $V_{\perp}^{max}(i)(> 0)$ on its vertical speed. Also assume $V_{\perp} \leq \min_i V_{\perp}^{max}(i)$.

A.5′ Aircraft of ith type has a lower bound $V_{\parallel}^{min}(i)(> 0)$ on its horizontal speed. Also assume $V_{\parallel} \geq \max_i V_{\parallel}^{min}(i)$.

A.6′ $L - \frac{2H_{sep}}{\min_i V_{\perp}^{max}(i)} V_{\parallel} \geq R.$

Let $\mathcal{E}'$ denotes the class of all encounters in which the initial state (relative positions and velocities when the conflict resolution maneuver is taken) satisfies A0, A.5′ and A.6′. If maneuver according to A.1-A.3 and A.4′ is taken to resolve an encounter in $\mathcal{E}'$, then we have

$$\min_{\mathcal{E}'}(L-R) = \frac{2H_{sep}}{\min_i V_{\perp}^{max}(i)} \max_i V_{\parallel}^{min}(i). \tag{3.3}$$

We use (3.3) and the characterisations in earlier section to obtain the PBC criteria given in Table 1.

PBC grades	grade 1	grade 2	grade 3
Scenario 1	$3H_{sep}$	$3H_{sep} + \frac{\min\limits_i V_\perp^{max}(i)}{\max\limits_i V_\parallel^{min}(i)} R$	$3H_{sep} + \frac{\min\limits_i V_\perp^{max}(i)}{\max\limits_i V_\parallel^{min}(i)} 2R$
Scenario 2	$2H_{sep}$	$2H_{sep} + \frac{\min\limits_i V_\perp^{max}(i)}{2\max\limits_i V_\parallel^{min}(i)} R$	$2H_{sep} + \frac{\min\limits_i V_\perp^{max}(i)}{\max\limits_i V_\parallel^{min}(i)} R$

Table 1: Minimum box height h_{min} for scenarios 1 and 2 with heterogeneous aircraft

4 Issues Related to the Width of a Rectangular Box

In the previous section, by considering a class of encounters we have derived sufficient conditions for the minimum box height to achieve *NNE* before some pre-specified stopping times. We are going to adopt a similar approach in order to derive a sufficient large width for the rectangular 3D box *PBC* of Section 3 i.e., $\vec{a}_1 = [d, 0, 0], \vec{a}_2 = [0, d, 0]$ and $\vec{a}_3 = [0, 0, h]$.

In order to derive a sufficient width for the rectangular box, we consider a horizontal resolution scenario between two aircraft, both of which maneuver. The scenario is presented in the form of following assumptions.

4.1 Assumptions of Scenario 3

We consider a large class of encounters concerning a pair of aircraft at the same flight level. First we state the assumptions adopted. Let L be the distance between them at time $t = 0$ when ASAS maneuver is started. i.e., $\|\tilde{s}_0^{12}\| = L$. Let $V_\parallel$ be the absolute value of their horizontal velocities.

Assumptions on initial state

B.0 Let there be two aircraft, #1 and #2 respectively flying at the same flight level and are on a head-on collision course with equal speed from opposite directions. At time zero there is no other aircraft within the horizontal separation minima of either of #1 and #2.

B.1 Aircraft of ith type has a lower bound $V_\parallel^{min}(i)(> 0)$ on its horizontal speed. Also assume $V_\parallel \geq \max\limits_i V_\parallel^{min}(i) = V_m$ (say).

Assumptions on maneuver

B.2 #1 and #2 start horizontal resolution simultaneously at $t = 0$.

B.3 Both of #1 and #2 turn left for a specific time interval with constant angular acceleration $\alpha_\vdash = g \tan\beta$ keeping the absolute value of the horizontal speed unchanged, where β is the constant banking angle of the aircraft (see Section 5.2).

B.4 No change of height.

4.2 Scenario 3 Predicted ASAS Horizontal Instantaneous Resolution

Under manoeuver constraint assumptions B.2, B.3 and B.4, both aircraft #1 and #2, when having an encounter B.0 and B.1, start resolution at the same time $t = 0$, and continue with constant

angular acceleration and constant speed till a pre-specified time t^*. After t^* each stops turning and follow a linear trajectory with constant horizontal speed. Since, both of the angular acceleration and the speed are constant, the radius of curvature is also constant. Therefore, each aircraft takes left turn by following a circular path of radius $r := \frac{V_\parallel^2}{\alpha_\vdash}$ and finally completes a turn of angle $\psi := \frac{t^* V_\parallel}{r}$ at t^*. Figure 4 demonstrates the predicted resolution. For this scenario we choose the minimum t^*

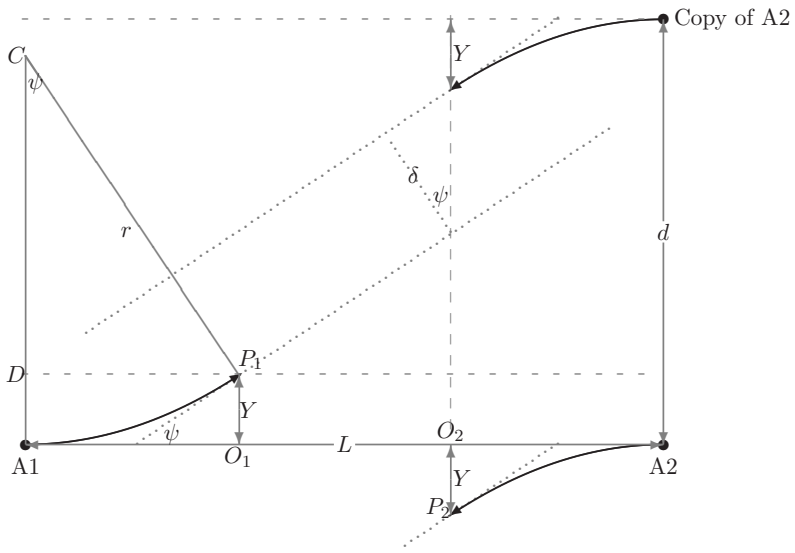

Figure 4: Top view of ASAS horizontal resolution (predictions)

or equivalently the minimum angle of turn ψ such that the horizontal separation between both of the aircraft is never less than the horizontal separation minima R, in case the other aircraft is not doing a resolution.

Let, the trajectories S_1^ψ and S_2^L be such that $S_1^\psi(0) = (0,0)$, $\dot{S}_1^\psi(t) = V_\parallel \left(\cos\left(\frac{V_\parallel}{r} t \bigwedge \psi\right), \sin\left(\frac{V_\parallel}{r} t \bigwedge \psi\right)\right)$ and $S_2^L(t) = (L - V_\parallel t, 0)$ where $a \bigwedge b$ denotes the minimum of two real numbers a and b. Given a separation minima R and initial distance L, #1 chooses a trajectory $S_1^{\psi_0}(t)$ such that

$$R = \min_t \|S_1^{\psi_0}(t) - S_2^L(t)\| > \min_t \|S_1^{\psi}(t) - S_2^L(t)\| \tag{4.4}$$

for any $\psi < \psi_0$, provided ψ_0 exists in $(0,\pi)$ for given R and L. We define $\mathcal{D}_r := \{(R,L) \in (0,\infty)\times(0,\infty) | \exists \psi_0 \in (0,\pi)$ such that $\min_t \|S_1^{\psi_0}(t) - S_2^L(t)\| = R$ holds with radius of curvature $r\}$. Hence, for $(R,L) \in \mathcal{D}_r$ there exists a unique ψ_0 satisfying (4.4) and hence the angle ψ_0 can be denoted as $\psi(R,L)$.

Theorem 4.1 *Assume,* $(R,L) \in \mathcal{D}_r$.
(i)Let t' *be the time instant of predicted miss distance between #1 and #2 i.e.,* $t' := \arg\min \|S_1^{\psi(R,L)}(t) - S_2^L(t)\|$, *then* $t' \geq \psi(R,L)\frac{r}{V_\parallel} = t^*$.
(ii) $t' = \psi(R,L)\frac{r}{V_\parallel} + \frac{1}{2V_\parallel}\left(L - r\psi(R,L) - 2r\tan\frac{\psi(R,L)}{2}\right)$.
(iii)$L - r\psi(R,L) \geq 2r\tan\frac{\psi(R,L)}{2}$.
(iv) Let $g_r(L,\psi) := (L - r\psi)\sin\frac{\psi}{2}$ *then* $\psi(R,L)$ *is the unique solution of* $g_r(L,\cdot) = R$.
(v) If $r \geq R/\sqrt{2}$, *then* $\psi(R,L) \leq \pi/2$.
(vi) Assume the constants r, R *and* L *satisfy the following relation* $L = r\psi(R,L) + 2r\tan\frac{\psi(R,L)}{2}$. *Then* $L = \min\{L' : (R,L') \in \mathcal{D}_r\}$.

Proof : (i) Let if possible $t' := \arg\min \|S_1^{\psi(R,L)}(t) - S_2^L(t)\| < \psi(R,L)\frac{r}{V_\parallel}$. Then we define $\psi' := \frac{V_\parallel}{r}t'$ which is less than $\psi(R,L)$. We can also define an alternative trajectory of #1 given by $S_1^{\psi'}(t)$. Since, $t' < \psi(R,L)\frac{r}{V_\parallel}$ we have $S_1^{\psi'}(t') = S_1^{\psi(R,L)}(t')$ as well as $\dot{S}_1^{\psi'}(t') = \dot{S}_1^{\psi(R,L)}(t')$ and hence

$$\frac{d}{dt}\|S_1^{\psi'}(t) - S_2^L(t)\|^2\Big|_{t=t'} = \frac{d}{dt}\|S_1^{\psi(R,L)}(t) - S_2^L(t)\|^2\Big|_{t=t'}.$$

Again from the definition of t' it is a local minima of $\|S_1^{\psi(R,L)}(t) - S_2^L(t)\|^2$ which implies that the right side of above equation is zero. This implies that t' is a local minima of $\|S_1^{\psi'}(t) - S_2^L(t)\|^2$ also. Thus, $\min_t \|S_1^{\psi'}(t) - S_2^L(t)\| = \|S_1^{\psi'}(t') - S_2^L(t')\| = \|S_1^{\psi(R,L)}(t') - S_2^L(t')\| = \min_t \|S_1^{\psi(R,L)}(t) - S_2^L(t)\| = R$. Hence contradicting (4.4) with $\psi' < \psi(R,L)$.

(ii) Let $S_{12}(t) := S_1^{\psi(R,L)}(t) - S_2^L(t)$ and $V_{12}(t) := \dot{S_{12}}(t)$. Therefore $S_{12}(\psi(R,L)\frac{r}{V_\parallel}) = (r\sin\psi(R,L) - L + r\psi(R,L), r(1-\cos\psi(R,L)))$ and $V_{12}(t) = V_\parallel(1+\cos\psi(R,L), \sin\psi(R,L))$ for all $t \geq \psi(R,L)\frac{r}{V_\parallel}$. Note that #1 takes rectilinear trajectory during $[\psi(R,L)\frac{r}{V_\parallel}, t']$ and $t' = \arg\min \|S_1^{\psi(R,L)} - S_2^L\|$. Therefore, the total distance traveled by both a/c during $[\psi(R,L)\frac{r}{V_\parallel}, t']$ = the total distance traveled by both a/c till miss distance achieved. Hence,

$$(t' - \psi(R,L)\frac{r}{V_\parallel})\|V_{12}\| = \frac{-S_{12}(\psi(R,L)\frac{r}{V_\parallel})\cdot V_{12}}{\|V_{12}\|}.$$

By substituting the value of $S_{12}(\psi(R,L)\frac{r}{V_\parallel})$ and V_{12} in the above equation we obtain

$$t' = \psi(R,L)\frac{r}{V_\parallel} + \frac{1}{2V_\parallel}\left(L - r\psi(R,L) - 2r\tan\frac{\psi(R,L)}{2}\right).$$

(iii) Follows from (i) and (ii).

(iv) Following the notation defined in the proof of (ii) we calculate

$$\min_t \|S_1^{\psi(R,L)} - S_2^L\| = \|S_{12}(t')\| = \|S_{12}(\psi(R,L)\frac{r}{V_\parallel}) + (t' - \psi(R,L)\frac{r}{V_\parallel})V_{12}\|$$

where t' is the time of miss distance. From the proof of (ii) we substitute the value of t', V_{12} and $S_{12}(\psi(R,L)\frac{r}{V_\parallel})$ in the above equation and we get

$$\min_t \|S_1^{\psi(R,L)} - S_2^L\| = (L - r\psi(R,L))\sin\frac{\psi(R,L)}{2}.$$

Again $g_r(L,\psi) := (L - r\psi)\sin\frac{\psi}{2}$. Therefore from above equation and (4.4) we have

$$\psi(R,L) = g_r(L,\cdot)^{-1}(R) \tag{4.5}$$

provided the inverse exists. From implicit function theorem we have the following. Let, (L_0,ψ_0) be such that $g_r(L_0,\psi_0) = R$ and $\frac{\partial}{\partial\psi}g_r(L_0,\psi_0) \neq 0$ then there is a open neighborhood U_{L_0} of L_0 such that a function $\psi(R,\cdot)$ can be defined on U_{L_0} as in (4.5). We have,

$$\frac{\partial}{\partial\psi}g_r(L,\psi) = \frac{1}{2}(L - r\psi)\cos\frac{\psi}{2} - r\sin\frac{\psi}{2}.$$

From (iii) it follows that $\frac{\partial}{\partial\psi}g_r(L,\psi(R,L)) \geq 0$. Clearly, $\frac{\partial}{\partial\psi}g_r(L',\psi(R,L')) = 0$ if and only if $L' - r\psi(R,L') = 2r\tan\frac{\psi(R,L')}{2}$. Hence, $\psi(R,L')$ is a solution of $R = g_r(L',\psi) = 2r\sin\frac{\psi}{2}\tan\frac{\psi}{2}$.

The right side is monotonic in ψ on $[0,\pi]$. Therefore, $\psi(R,L')$ is the unique solution of the above equation $R = 2r\sin\frac{\psi}{2}\tan\frac{\psi}{2}$. Thus, $\psi(R,L)$ is the unique solution of $R = g_r(L,\cdot)$ for all $(R,L) \in \mathcal{D}_r$.

(v) From (iii) and (iv) we have $2r\tan\frac{\psi(R,L)}{2}\sin\frac{\psi(R,L)}{2} \le R$. If $r \ge R/\sqrt{2}$, we have $\tan\frac{\psi(R,L)}{2}\sin\frac{\psi(R,L)}{2} \le 1/\sqrt{2} = \tan\frac{\pi}{4}\sin\frac{\pi}{4}$. Since the function on left is monotone increasing in ψ on the interval $[0,\pi/2]$, we have $\psi(R,L) \le \pi/2$.

(vi) From (iv) we get $\frac{\partial\psi(R,L)}{\partial L}(\frac{L}{2}\cos\frac{\psi(R,L)}{2} - r(\sin\frac{\psi(R,L)}{2} + \frac{\psi(R,L)}{2}\cos\frac{\psi(R,L)}{2})) = -\sin\frac{\psi(R,L)}{2}$. Using the inequality in (iii) we have,

$$\frac{\partial\psi(R,L)}{\partial L} < 0. \tag{4.6}$$

Or in other words $\psi(R,L)$ is a strictly decreasing function on L. If possible we assume that there are $L' < L''$ such that $(R,L') \in \mathcal{D}_r$, $(R,L'') \in \mathcal{D}_r$ and $L'' = r\psi(R,L'') + 2r\tan\frac{\psi(R,L'')}{2}$. Then from (4.6) we get $L' < r\psi(R,L') + 2r\tan\frac{\psi(R,L')}{2}$ which contradicts (iii). Therefore, $L'' = \min\{L' : (R,L') \in \mathcal{D}_r\}$. ∎

Theorem 4.2 *Consider the following system with $R > 0$ and $r(> R/\sqrt{2})$*

$$(L - r\psi)\sin\frac{\psi}{2} = R \tag{4.7}$$

$$r\psi + 2r\tan\frac{\psi}{2} = L. \tag{4.8}$$

(i) The system (4.7)-(4.8) has a unique solution (L^*,ψ^*) (say).
(ii) $(R,L^*) \in \mathcal{D}_r$.
(iii) $\psi^* = \psi(R,L^*)$.
(iv) $L^* = \min\{L : (R,L) \in \mathcal{D}_r\}$.

Proof : (i) For $r > R/\sqrt{2} > 0$, the equation $2r\sin\frac{\psi}{2}\tan\frac{\psi}{2} - R = 0$ has a unique solution in $(0,\pi/2)$. Let ψ^* be the solution and we also define $L^* := r\psi^* + 2r\tan\frac{\psi^*}{2}$. Clearly, (L^*,ψ^*) is the unique solution of the system (4.7)-(4.8).

(ii) We can show that $\min_t \|S_1^{\psi^*} - S_2^{L^*}\| = \|S_1^{\psi^*}(\psi^*\frac{r}{V_\parallel}) - S_2^{L^*}(\psi^*\frac{r}{V_\parallel})\| = (L^* - r\psi^*)\sin\frac{\psi^*}{2} = R$. Hence, $(R,L^*) \in \mathcal{D}_r$.

(iii) From (ii) of Theorem 4.2 and (iv) of Theorem 4.1 we have $\psi(R,L^*)$ is the unique solution of $g_r(L^*,\psi) = R$. Again in (i) of Theorem 4.2 we showed $g_r(L^*,\psi^*) = R$. Thus $\psi^* = \psi(R,L^*)$.

(iv) Follows from (i), (ii), (iii) of Theorem 4.2 and (vi) of Theorem 4.1. ∎

In view of the above two theorems we consider the following additional assumptions on the initial state:

B.5 (i) $r = \frac{V_\parallel^2}{\alpha_\vdash} > \frac{R}{\sqrt{2}}$ and (ii) $L \ge L^*$ where L^* is as in Theorem 4.2.

We define a stopping time τ' as the time instant of predicted miss distance between #1 and the copy of #2 in the neighboring box on its right. We look for a rectangular box which is sufficiently large with respect to the set of encounters and maneuver constraint given in B.0-B.5 and the stopping time τ'.

4.3 Evaluation of Width of sufficiently large 3D box under scenario 3

Let in Figure 4, $r = \frac{V_\parallel^2}{\alpha_\vdash}$ be the radius of curvature of the circular path of #1 and $\psi = \psi(R, L)$. Therefore in the figure aircraft #i completes circular path at the point P_i. Subsequently, it continues with zero acceleration by following a linear trajectory which is tangent to the curvilinear path at point P_i. This tangent also makes angle ψ with the pre-maneuver predicted trajectory. Let O_i be the orthogonal projection of P_i on the line of pre-maneuver predicted trajectory. If the coordinate of P_1 is (X, Y), then $\overline{A_1O_1} = \overline{A_2O_2} = X$. Hence $\overline{O_1O_2} = L - 2X$. Therefore, the predicted miss distance δ, between the predicted trajectories of #1 and the copy of #2 in the neighboring box on right side of #2 is given by

$$\begin{aligned} \delta &= (d - 2Y - \overline{O_1O_2}\tan\psi)\cos\psi \\ &= (d - 2Y - (L - 2X)\tan\psi)\cos\psi \end{aligned}$$

where d is the side lengths of the box. To obey *NNE* during $[0, \tau']$ we must have $\delta \geq R$ for all encounters satisfying B.0 - B.5. Thus we get

$$(d - 2Y - (L - 2X)\tan\psi(R, L))\cos\psi(R, L) \geq R \tag{4.9}$$

for all $L \geq L^*$ and $V_\parallel \geq V_m$ with $\psi(R, L)$ unique solution of $g_r(L, \cdot) = R$. From the figure we calculate $X = r\sin\psi(R, L)$ and $Y = r - r\cos\psi(R, L)$. We also have $r = \frac{V_\parallel^2}{\alpha_\vdash}$. Hence from (4.9) we have

$$\begin{aligned} d &\geq \max_{V_\parallel \geq V_m} \max_{L \geq L^*} \left(\frac{R}{\cos\psi(R, L)} + 2\frac{V_\parallel^2}{\alpha_\vdash}(1 - \cos\psi(R, L)) + (L - 2\frac{V_\parallel^2}{\alpha_\vdash}\sin\psi(R, L))\tan\psi(R, L) \right) \\ &= d^*(\text{say}) \end{aligned} \tag{4.10}$$

It is important to note that, the assumption in B.0* is not checked yet. To derive the above condition we have considered the copy of A2 on its right side only. The position of the copy of A2 on its left side is not relevant because in B.3 the left turns are assumed. But still the position of copy of A2 just behind A1 has an important role in validating our analysis. Though this copy would fly away of A1 but its initial separation should be larger than the horizontal separation minima according to B.0*. Therefore, we obtain another condition on the initial separation L of A1 and A2 namely,

$$L \leq d - R. \tag{4.11}$$

Thus B.0-B.5 along with (4.11) represents a nonempty class of encounters if and only if $L^* \leq d - R$ or equivalently, $d \geq L^* + R$. Let

$$d_{\min} := \max(d^*, L^* + R),$$

then $d \geq d_{\min}$ gives a necessary and sufficient condition of width for the 3D box. If the box width d is greater or equal to $d_{\min}$ as derived above, the box is sufficiently large for simulating the encounters with maneuver constraints listed in B.0-B.5.

5 Numerical Evaluation

5.1 3D Box Height

Homogeneous aircraft

We consider the speed constraints of several aircraft types and altitudes from BADA 3.6 Performance Files (ref : Aircraft performance summary tables for the base of aircraft data (BADA),

revision 3.6, Eurocontrol). The details are given in Appendix A. The data presented in Appendix A shows that the value of climb parameter $\frac{V_{\perp}^{max}}{V_{\parallel}^{min}}$ ranges roughly from 0.05 to 0.08 depending on the aircraft type. Since the expressions of suggested minimum box height of grade 3, i.e., $h_{\min}$ (calculated in earlier sections) involves the climb parameter, we illustrates the dependence of $h_{\min}$ (for the homogeneous case) on the value of climb parameter by the following plots in Figure 5. The

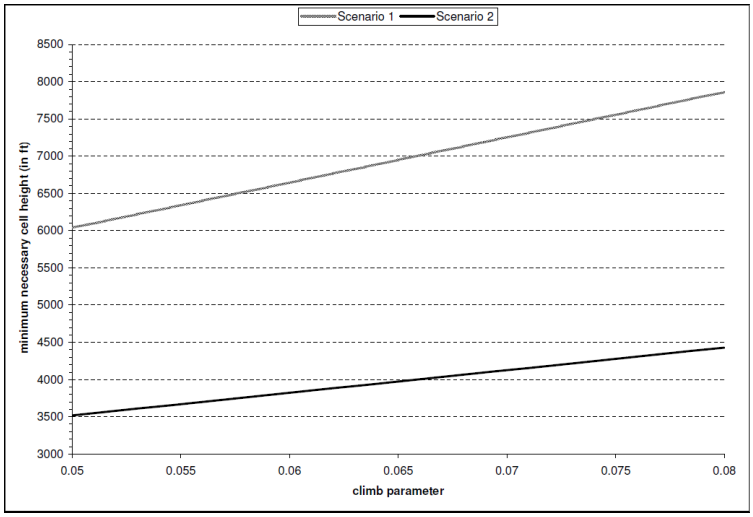

Figure 5: h_{min} required for a grade 3 PBC as a function of $\frac{V_{\perp}^{max}}{V_{\parallel}^{min}}$ for scenarios 1 and 2

parameter values are plotted along horizontal axis and the corresponding evaluation of $h_{\min}$ (using (3.1) and (3.2)) is plotted along vertical axis. In particular we take $R = 5Nm = 30380.57743$ft and $H_{sep} = 1000$ft. The graph comprises the result of two different scenarios discussed in Subsections 3.3 and 3.4.

Heterogeneous aircraft

Next we evaluate the minimum sufficient height of the 3D box in heterogeneous random traffic airspace model for both the scenarios. We obtain the numerical values from tables in Appendix B. In the tables the velocity constraints of five different types of aircraft are given for their positions in three different flight levels. We assume that these are the variety of aircraft in the heterogeneous random traffic airspace model that we consider. In reality, the horizontal encounters may happen with aircraft only in the same flight level. Therefore, it seems that the constraint for a different flight level has no influence in resolving the current encounter. But under periodic boundary conditions all the copies of an aircraft in vertical direction have same velocities. Therefore under *PBC* the effective velocity constraints are obtained by taking common constraint for all the flight levels. These constraints of the five different aircraft are given in Table 2. From Table 2 it follows that, for our

No.	Ac Type	Class	$V_{\perp}^{max}$ (fpm)	$V_{\parallel}^{min}$ (kts)	$\frac{V_{\perp}^{max}}{V_{\parallel}^{min}}$
1	A320-212	M	2700	458	0.058218504
2	A340-313	H	2160	469	0.04548243
3	B733 (B737-300)	M	2780	434	0.063258344
4	B744 (B747-400)	H	3060	493	0.061296723
5	B764 (B767-400)	H	2590	458	0.055846639

Table 2: Velocity constraints of five different aircraft under *PBC*

case $\min_i V_\perp^{max}(i) = 2160$ fpm and $\max_i V_\parallel^{min}(i) = 493$ kts. Therefore, $\dfrac{\min_i V_\perp^{max}(i)}{\max_i V_\parallel^{min}(i)} = 0.043268275$.

Using this, the numerical evaluation of Table 1 is given in Table 3.

PBC grades	grade 1	grade 2	grade 3
Scenario 1	3000 ft	4315 ft	5629 ft
Scenario 2	2000 ft	2657 ft	3315 ft

Table 3: Evaluation of Minimum rectangular box height h_{min} (in ft) for scenarios 1 and 2 with heterogeneous aircraft

By considering heterogeneous aircraft we find the minimum 3D box height. For scenarios 1 and 2 this yields two values for $h_{\min}$: 5629 ft and 3315 ft respectively. The height value used in [1] was 4000 ft, which is sufficiently large for scenario 2, but not for scenario 1. Adherence to the value of 5629 ft should have avoided the problem reported in example 2.6 where two aircraft behaved like scenario 1.

5.2 3D Box Width

The angular acceleration($\alpha_\vdash$) of the aircraft depends on its banking angle β so that with reference to the aircraft the parallel component of centrifugal force is balanced with parallel component of the gravitational force. In particular, the relation is

$$\alpha_\vdash = g \tan \beta$$

where g is the gravitational acceleration (assumed to be the same for all height). For civil aircraft $\beta \in [0, \pi/6]$. For $\beta = \pi/6$ we calculate

$$\alpha_\vdash \geq g \tan \frac{\pi}{6} = 5.663806141 m/s^2. \tag{5.12}$$

We consider the heterogeneous scenario with aircraft types as in Appendix A. From Table 5.2 $V_m = 493kts = 253.5992m/s$. We also take $R = 5Nm = 9260m$. Thus we have $r = \frac{V_m^2}{\alpha_\vdash} \geq 11355.07791m > R/\sqrt{2}$. Therefore, the assumption in Theorem 4.2 is valid. The computation of $d_{\min}$ involves a maximization problem (4.10) which has to be done numerically. To this end we determine the domain of maximization. By solving the system (4.7)-(4.8) we obtain

$$\psi^* = 2 \cos^{-1} \left(\frac{4r}{R + \sqrt{R^2 + 16r^2}} \right). \tag{5.13}$$

Given a value of $V_\parallel \geq V_m$ we find $r = \frac{V_\parallel^2}{\alpha_\vdash}$ using (5.12) and we substitute this value in (5.13) to get the value of ψ^*. Next L^*, the lower bound of variable L is obtained from (4.8) by substituting $\psi = \psi^*$. Then the inner maximum of (4.10) is computed for the given value of $V_\parallel$. Finally the value of d^* is obtained by numerical computation of outer maximum over all $V_\parallel \geq V_m$. The following table shows the computation of $d_{\min}$ for different bank angles.

Bank angle β	Radius of curvature $r \geq$	Corresponding ψ^*	Corresponding L^*	d^*	$d_{\min} = \max(d^*, L^* + R)$
30^o	11.37 km	70.45^o	16.2 Nm	36.2 Nm	36.2 Nm
25^o	14.07 km	63.81^o	17.9 Nm	28.5 Nm	28.5 Nm

Table 4: Heterogeneous model: Computation of $d_{\min}$ for different bank angles and $V_m = 493kts$

Since it is of interest to know what happens to the box width at other V_m values, we also calculate $d_{\min}$ with a smaller and higher value of V_m (see Tables 5 and 6).

Bank angle β	Radius of curvature $r \geq$	Corresponding ψ^*	Corresponding L^*	d^*	$d_{\min}$ $= \max(d^*, L^* + R)$
30^o	9.81 km	75.35^o	15.15 Nm	46.4 Nm	46.4 Nm
25^o	12.15 km	68.33^o	16.73 Nm	33.2 Nm	33.2 Nm

Table 5: Heterogeneous model: Higher $d_{\min}$ for a smaller $V_m = 458kts$

Bank angle β	Radius of curvature $r \geq$	Corresponding ψ^*	Corresponding L^*	d^*	$d_{\min}$ $= \max(d^*, L^* + R)$
30^o	15.9 km	60.2^o	18.99 Nm	25.9 Nm	25.9 Nm
25^o	19.7 km	54.4^o	21.04 Nm	22.7 Nm	26.0 Nm

Table 6: Heterogeneous model: Lower $d_{\min}$ for a higher $V_m = 583kts$

In [1], $V_m = 493kts$ and 25^o maximum bankangle has been used and a PBC width of 40Nm. Table 4 shows that this width was sufficiently large and might even be reduced to 30Nm.

6 Conclusion

In [1], a very large 3D airspace with a very large number of airborne self separating aircraft have been simulated by making use of a Periodic Boundary Condition (PBC) [4]. The specific PBC used is a rectangular 3D box, which are packing a virtually infinite 3D airspace. In each 3D box, N airborne self separating aircraft are flying. This way, one only needs to simulate N aircraft in one box, in order to mimic a simulation of infinitely many aircraft in an infinite 3D airspace. The maximum number of aircraft that has been simulated without running into computer memory problems was $N = 8$. Subsequently, the size of the 3D box has been varied in order to vary the aircraft density in the 3D airspace.

Although the use of PBC is a well known approach in physics particle simulation, little is known about choosing a sufficiently large PBC. Therefore in [1] the size of the 3D box has been chosen rather arbitrarily, and it subsequently has been observed that sometimes a rare event happened in the simulation which was due to the limited size of the 3D box. Because events caused by the limited size of the 3D box can properly be identified, the potential errors caused by a too small sized 3D box can be kept under control. In order to better understand under which conditions the size of the 3D box is large enough, this report has derived bounds on the size of the 3D boxes under the airborne self separation concept considered in [1].

Some sufficient conditions for the minimum box height h_{min} have been derived in Section 3 for use in PBC towards collision risk simulation for the airborne self separation concept considered in [1]. The derivations also indicate the possible consequences of a simulation model with PBC having 3D box height below h_{min}. Similarly, in section 4 we derived the minimum sufficient 3D box width d_{min}. In section 5 values for h_{min} and d_{min} have been evaluated and these appear to be higher and lower than those used in [1] (see Example 2.5.). Therefore the present study opens up the scope of increasing the height and decreasing the width of the 3D box.

For the concept considered in [1] the derivations developed in this report have shown that a PBC defined by a 3D rectangular box of height 6000 ft and width of 30 Nm would be sufficiently large to simulate an infinitely large airspace. Because the 3D rectangular box used in [1] was 4000 feet high and 40 NM width, this explains why collisions have been reported which were caused by a too small height of the 3D box. The operational concept considered within iFly differs significantly

from the one considered in [1], there is no certainty yet whether a PBC using similar rectangular 3D box works as well as it has shown to work in [1]. Hence it remains to try this out in WP7.3 foreseen large scale MC simulations of an advanced airborne self separation concept, and we should be prepared in identifying undesired events that are caused by the use of a 3D rectangular box as PBC.

References

[1] Henk A. P. Blom, Bart Klein Obbink and G. J. Bakker, *Simulated collision risk of an uncoordinated airborne self separation concept of operation*, 7th Eurocontrol Innovative Research Workshop, Bretigny, December 2-4, 2008.

[2] M.H.C Everdij, G.J. Bakker and H. A. P. Blom, *CARE/ASAS Activity 3: Airborn Separation Minima - WP3 report: Estimating safe separation*, Version 2.0, January 2002.

[3] B. Klein Obbink, *Description of advanced operation: Free Fligft*, Distributed Control and Stochastic Analysis of Hybrid Systems Supporting Safety Critical Real-Time Systems Design.

[4] D. C. Rapaport, *The Art of Molecular Dynamics Simulation*, Second edition, Cambridge University Press, 2004.

[5] *Aircraft performance summary tables for the base of aircraft data (BADA)*, revision 3.6, Eurocontrol

A Appendix: BADA performance data

This appendix provides an overview of performance data used for several aircraft types from BADA 3.6 Performance Files [5].

Unit	Stands for	In SI units
ft	Feet	0.3048 (m)
FL	Flight Level	100ft (m)
fpm	Feet per minute	ft/60 (m/s)
kts	Knots	0.5144 (m/s)

Abbreviations:
Class : Heavy (H) or Medium (M)
ROC :Rate Of Climb
ROD :Rate Of Descend
TAS : True Airspeed

From BADA 3.6:

Values for FL 220

Ac Type	Class	Max(ROC, ROD) (fpm)	Min(TAS) (kts)	Factor Max (ROC,ROD) / Min(Tas)
A320-212	M	2700	425	0.0627
A340-313	H	2160	412	0.0518
B733 (B737-300)	M	2780	386	0.0711
B744 (B747-400)	H	3120	464	0.0664
B764 (B767-400)	H	2780	399	0.0688

Values for FL 310

Ac Type	Class	Max(ROC, ROD) (fpm)	Min(TAS) (kts)	Factor Max (ROC,ROD) / Min(Tas)
A320-212	M	3540	458	0.0763
A340-313	H	2900	469	0.0611
B733 (B737-300)	M	3310	434	0.0753
B744 (B747-400)	H	3570	493	0.0715
B764 (B767-400)	H	2990	458	0.0645

Values for FL 420

Ac Type	Class	Max(ROC, ROD) (fpm)	Min(TAS) (kts)	Factor Max (ROC,ROD) / Min(Tas)
A320-212	M	-	-	-
A340-313	H	2340	459	0.0503
B733 (B737-300)	M	-	-	-
B744 (B747-400)	H	3060	482	0.0627
B764 (B767-400)	H	2590	447	0.0572